

Geometric Aspects of Composite Pulses

BY TSUBASA ICHIKAWA^{1†}, MASAMITSU BANDO¹, YASUSHI KONDO^{1,2} AND
MIKIO NAKAHARA^{1,2}

¹*Research Center for Quantum Computing,
Interdisciplinary Graduate School of Science and Engineering, Kinki University,
3-4-1 Kowakae, Higashi-Osaka, Osaka 577-8502, Japan*

²*Department of Physics, Kinki University,
3-4-1 Kowakae, Higashi-Osaka, Osaka 577-8502, Japan*

Unitary operations acting on a quantum system must be robust against systematic errors in control parameters for reliable quantum computing. Composite pulse technique in nuclear magnetic resonance (NMR) realises such a robust operation by employing a sequence of possibly poor quality pulses. In this article, we demonstrate that two kinds of composite pulses, one compensates for a pulse length error in a one-qubit system and the other compensates for a J -coupling error in a two-qubit system, have vanishing dynamical phase and thereby can be seen as geometric quantum gates, which implement unitary gates by the holonomy associated with dynamics of cyclic vectors defined in the text.

Keywords: NMR, Composite pulses, Geometric phases, Geometric quantum gates, Quantum control

1. Introduction

Nuclear magnetic resonance (NMR) has developed many techniques to control physical systems and maintain their coherence [1, 2]. A composite pulse is one of such techniques, in which a sequence of pulses is employed to cancel out a systematic error inherent in the pulses [3]. A systematic error is an unwanted imperfection in control parameters, such as poor calibration, and should not be confused with a random noise. The composite π -pulse by Levitt and Freeman [4], developed with intuitive but convincing account of its robustness, opened up a new field of research. Now we have hundreds of composite pulses [5, 6] and dozens of methods to design them, such as iterative expansion [7], gradient ascent pulse engineering (GRAPE) [8, 9] and concatenation [10].

Recently, quantum information processing (QIP) [12, 13, 14, 15] has an influence over the composite pulse design. Very accurate control of a quantum system is required for a successful quantum error correction, as shown in [14] for example. Any quantum algorithm can be simulated by quantum circuits composed of one-qubit unitary operations and the controlled-NOT (CNOT) operations. As a result, robustness is required for *arbitrary* one-qubit operations and CNOT operation. In contrast, operations with limited angles and phases have been required in conventional NMR manipulations. Numerous composite pulses have been proposed to date in the context of QIP [10, 16, 17, 18, 19, 20, 21, 22, 23].

[†] Present address: Department of Physics, Gakushuin University, 1-5-1 Mejiro, Toshima-ku, Tokyo 171-8588, Japan

Geometric quantum computation [24, 25] has been proposed to attain reliable quantum control. In addition to the dynamical phase, cyclic evolution of a quantum system allows for various geometric phases [26, 27, 28, 29, 30], which are controllable and thereby can be utilised for unitary operations. We call a gate implemented with a geometric phase a geometric quantum gate (GQG) hereafter. Mathematically, a geometric phase is regarded as a holonomy associated with a closed path in a suitable base manifold associated with a cyclic evolution [31, 32, 33]. Random fluctuations along the integration path are expected to cancel out, leading to a quantum gate robust against random noise. Although there is numerical support for the robustness of GQGs [34], this issue is still under debate [35].

In this article, we unite these two apparently different constructions of robust unitary operations. More precisely, we reveal that composite pulses robust against certain kinds of systematic errors are nothing but GQGs. This has been observed previously in one-qubit operations [36]. Now we elaborate and generalise this observation to two-qubit operations, which are indispensable for a universal set of quantum gates in QIP. Our work reveals that many composite pulses are geometric in nature and their robustness is attributed to the robustness of GQGs against certain errors.

This article is organised as follows. Geometric phase, in particular Aharonov-Anandan phase and its application to implementation of a quantum gate are introduced in Sec. 2. We employ the perturbation theory as a guiding principle to design composite pulses and derive the robustness condition in Sec. 3. In Sec. 4, we present the main statement of this article, that is, existing composite pulses to suppress the pulse length error and the J -coupling error are GQGs. We will employ a group theoretical argument to present our statement in a unified manner. The assertion in Sec. 4 is exemplified in Sec. 5 and 6 by analysing various composite pulses from our viewpoint. Section 7 is devoted to conclusion and discussions.

2. Geometric Quantum Gates

Geometric phase, anticipated in many branches of physics and chemistry [26], was formulated first by Berry in an adiabatic evolution of a quantum system. In [27], Berry considered a cyclic evolution of a quantum system whose Hamiltonian has time-dependent parameters, and pointed out that after the cyclic and adiabatic evolution, the system may acquire not only the dynamical phase factor, but also a geometric phase factor, which is given by a circuit integral in the parameter manifold. This integral is geometric, in the sense that it is independent of how fast the circuit is traversed. The Berry phase has been generalised in many ways. One of such generalizations is Wilczek-Zee holonomy: In the presence of n -fold degeneracy, the geometric phase factor can be replaced to an element of a unitary group $U(n)$, which is also independent of how fast the circuit is traversed [28].

Aharonov and Anandan showed in [29] that the geometric phase appears even in a non-adiabatic evolution. Consider an n -level system, whose normalised state vector at time $t \in [0, T]$ is given by $|\psi(t)\rangle \in \mathbb{C}^n$. Dynamics of the system is characterised by the Schrödinger equation

$$i \frac{d}{dt} |\psi(t)\rangle = H(\lambda(t)) |\psi(t)\rangle, \quad (2.1)$$

where the Hamiltonian $H(\lambda(t))$ is Hermite and time-dependent through parameters $\lambda(t) = (\lambda_1(t), \dots, \lambda_N(t))$. Here we set $\hbar = 1$. When the evolution is cyclic with a period T , i.e.,

$$|\psi(T)\rangle = e^{i\gamma} |\psi(0)\rangle, \quad \gamma \in \mathbb{R}, \quad (2.2)$$

then the phase γ the system acquires after the cyclic evolution includes geometric contribution γ_g , which is defined in terms of the dynamical phase γ_d as

$$\gamma_g = \gamma - \gamma_d, \quad \gamma_d = - \int_0^T dt \langle \psi(t) | H(\lambda(t)) | \psi(t) \rangle. \quad (2.3)$$

This phase γ_g is called the Aharonov-Anandan phase. It is possible to interpret the Aharonov-Anandan phase in terms of geometric structure of the Hilbert space \mathbb{C}^n . See Appendix A for details. Also, for another expression of the Aharonov-Anandan phase, see, *e.g.*, [29, 30, 33].

Applications of geometric phases are found in QIP. For example, Zanardi and Rasetti proposed to use the Wilczek-Zee holonomy to implement unitary gates [24]. It is also possible to implement unitary gates by using the Aharonov-Anandan phase [10, 25, 36, 37, 38]. To see this, let $\{|\psi_a\rangle\}_{1 \leq a \leq n}$ be the eigenvectors of a Hamiltonian $H(\lambda(0))$ and suppose their dynamical evolution is cyclic, that is,

$$|\psi_a(T)\rangle = U(T) |\psi_a\rangle, \quad U(T) = \mathcal{T} e^{-i \int_0^T ds H(\lambda(s))} \quad (2.4)$$

and

$$|\psi_a(T)\rangle = e^{i\gamma^a} |\psi_a\rangle, \quad \gamma^a \in \mathbb{R}, \quad (2.5)$$

where the time-ordered product is denoted by \mathcal{T} . Equating Eqs. (2.5) and (2.4), we observe that $|\psi_a\rangle$ is an eigenvector of $U(T)$ with the eigenvalue $e^{i\gamma^a}$, that is,

$$U(T) |\psi_a\rangle = e^{i\gamma^a} |\psi_a\rangle. \quad (2.6)$$

When there is no degeneracy, the spectral decomposition of $U(T)$ is written as

$$U(T) = e^{i\gamma^1} |\psi_1\rangle \langle \psi_1| + \dots + e^{i\gamma^n} |\psi_n\rangle \langle \psi_n|. \quad (2.7)$$

The phase γ^a is decomposed as $\gamma^a = \gamma_g^a + \gamma_d^a$ in terms of the dynamical phase defined as

$$\gamma_d^a = - \int_0^T dt \langle \psi_a(t) | H(\lambda(t)) | \psi_a(t) \rangle, \quad |\psi_a(t)\rangle = U(t) |\psi_a\rangle. \quad (2.8)$$

A unitary operator $U(T)$ is called a geometric quantum gate (GQG) if γ_d^a vanishes for all a .

3. Perturbative Construction of Composite Pulses

In actual situations in NMR, the dynamics is controlled by a sequential application of rf-pulses with constant field strength. Accordingly, the time interval $[0, T]$ is divided into k intervals, in each of which the Hamiltonian is constant. More precisely,

we define the i -th temporal interval $[t_{i-1}, t_i]$, where t_i satisfies $0 = t_0 < t_1 < \dots < t_k = T$, and define a piecewise constant Hamiltonian, which takes the form $H(\lambda^i)$ in the i -th interval $[t_{i-1}, t_i]$. Here $\lambda^i = (\lambda_1^i, \dots, \lambda_N^i)$ is a constant parameter vector while N is the number of control parameters. Then, the i -th rf-pulse gives rise to a unitary operator

$$e^{-iW^i}, \quad W^i = H(\lambda^i) \cdot (t_i - t_{i-1}), \quad (3.1)$$

and $U(T)$ can be written as

$$U(T) = e^{-iW^k} \dots e^{-iW^1}. \quad (3.2)$$

Now we wish to implement a ‘target’ unitary operator U as $U = U(T)$. The target U should be implemented in a way robust against the error under consideration as much as possible. Hereafter we seek a condition for such robust implementation.

We consider errors which cause displacement

$$W^i \rightarrow W^i + \delta W^i, \quad (3.3)$$

where δW^i is a self-adjoint operator corresponding to the error. When δW^i is sufficiently small in the sense of the operator norm, we can use the perturbation theory and find

$$e^{-i(W^i + \delta W^i)} \approx e^{-iW^i} (\mathbb{1}_n - i\delta W_I^i); \quad \delta W_I^i := \int_0^1 dx e^{ixW^i} \delta W^i e^{-ixW^i}, \quad (3.4)$$

to the first order in δW^i . Here the identity operator on \mathbb{C}^n is denoted by $\mathbb{1}_n$. The operator δW_I^i is the error operator δW^i in the interaction picture. Then, the unitary operator U' implemented with the error δW^i is given by

$$U' = e^{-i(W^k + \delta W^k)} \dots e^{-i(W^1 + \delta W^1)} \approx U (\mathbb{1}_n - i\Delta W), \quad (3.5)$$

where

$$\Delta W = \sum_{i=1}^k V^{i-1 \dagger} \delta W_I^i V^{i-1}, \quad V^i = e^{-iW^i} \dots e^{-iW^1} \quad \text{for } i = 1, 2, \dots, k-1, \quad (3.6)$$

with $V^0 = \mathbb{1}$. Many, albeit not all, composite pulses satisfy the following robustness condition

$$\Delta W = 0, \quad (3.7)$$

which we can evaluate once we specify δW^i . This condition guarantees the effect of the error vanishes to the first order in δW^i .

Now we wish to address the relation between the robustness condition (3.7) and a classification of composite pulses common in the NMR community. There are two types, Type A and Type B, of composite pulses [5, 16]. The error tolerance is independent of the initial state vector for Type A composite pulses, whereas it is not the case for Type B composite pulses. In view of this, the composite pulses satisfying (3.7) are clearly of Type A.

4. Composite Pulses as Geometric Quantum Gates

To see the geometric nature of Type A composite pulses, we follow the argument introduced in [36], which has been generalised to multi-qubit system in [10]. Suppose that the systematic error is proportional to W^i :

$$\delta W^i = \epsilon W^i. \quad (4.1)$$

As shown later, two kinds of systematic errors are of this form. The robustness condition (3.7) reads

$$\Delta W = \epsilon \sum_{i=1}^k V^{i-1\dagger} W^i V^{i-1} = 0, \quad (4.2)$$

where use has been made of the identity $\delta W_I^i = \delta W^i$ derived from Eq. (3.4) and Eq. (4.1). Taking the expectation value of ΔW with respect to $|\psi_a\rangle$, we obtain

$$\gamma_d^a = \sum_{i=1}^k \gamma_d^a(i) = 0, \quad \gamma_d^a(i) := -\langle \psi_a(i-1) | W^i | \psi_a(i-1) \rangle, \quad (4.3)$$

where $|\psi_a(i)\rangle := V^i |\psi_a\rangle$. Hence, any composite pulse which is designed by the perturbation theory and compensates the error (4.1) is GQG. In what follows, we will show that composite pulses associated with two kinds of relevant systematic errors are GQGs.

(a) Error on One-Qubit System

We turn to a one-qubit system, whose Hilbert space is \mathbb{C}^2 . An SU(2) operations we can implement with a single rf-pulse in NMR is limited to the form

$$W^i = \theta_i \mathbf{n}_i \cdot \boldsymbol{\sigma} / 2, \quad (4.4)$$

where $\mathbf{n}_i = (\cos \phi_i, \sin \phi_i, 0)$ and $\boldsymbol{\sigma} = (\sigma_x, \sigma_y, \sigma_z)$ due to the apparatus limitation. Nevertheless, we can implement any SU(2) operation by combining at most three such pulses using the Euler angle decomposition [12, 15]. The displacement (3.3) under the error (4.1) is seen as

$$\theta_i \rightarrow (1 + \epsilon) \theta_i. \quad (4.5)$$

This is a well-known systematic error called the pulse length error in the NMR community [5]. Hence, from the previous argument, we observe that any composite pulse compensating for the pulse length error is a GQG.

(b) Error in Two-Qubit System

For a two-qubit system, the relevant Hilbert space and the set of unitary operations are $\mathbb{C}^{2 \otimes 2}$ and SU(4), respectively. In view of quantum information processing, the controlled-NOT (CNOT) operation

$$U_{\text{CNOT}} = |0\rangle\langle 0| \otimes \mathbb{1}_2 + |1\rangle\langle 1| \otimes \sigma_x \quad (4.6)$$

is important.[†] Here, $|a\rangle \in \mathbb{C}^2$ with $a = 0, 1$ is the eigenvector of σ_z with the eigenvalue $(-1)^a$. The relevance of CNOT operation originates from the fact that any QIP can be implemented as a quantum circuit composed of one-qubit unitary operations and CNOT operations [11, 12, 15].

By using the Cartan decomposition [15], CNOT operation can be rewritten as $U_{\text{CNOT}} = K_1 H K_2$, with

$$H = e^{i\alpha_x \sigma_x \otimes \sigma_x} e^{i\alpha_y \sigma_y \otimes \sigma_y} e^{i\alpha_z \sigma_z \otimes \sigma_z} \quad K_1, K_2 \in \text{SU}(2) \otimes \text{SU}(2). \quad (4.7)$$

Since $\sigma_x \otimes \sigma_x$ is generated from $\sigma_z \otimes \sigma_z$ through the following identity

$$e^{i\alpha_x \sigma_x \otimes \sigma_x} = e^{i\pi(\sigma_y \otimes \mathbb{1}_2 + \mathbb{1}_2 \otimes \sigma_y)/4} e^{i\alpha_x \sigma_z \otimes \sigma_z} e^{-i\pi(\sigma_y \otimes \mathbb{1}_2 + \mathbb{1}_2 \otimes \sigma_y)/4}, \quad (4.8)$$

the Ising-type Hamiltonian

$$H = J\sigma_z \otimes \sigma_z/4 \quad (4.9)$$

is essential to implement CNOT operations which is commonly realised in a weak coupling limit. Hereafter we shall be concerned with the J -coupling error defined by

$$J \rightarrow (1 + \epsilon)J. \quad (4.10)$$

Several composite pulses robust against the J -coupling error have been proposed assuming that one-qubit operations are free from errors. These existing composite pulses [17, 18, 19, 20] are designed by making use of the following three generators only:

$$X := \sigma_z \otimes \sigma_z, \quad Y := \sigma_z \otimes \sigma_x, \quad Z := \mathbb{1}_2 \otimes \sigma_y, \quad (4.11)$$

among the fifteen generators of $\text{SU}(4)$. Evidently these operators satisfy $\mathfrak{su}(2)$ algebra:

$$[X/2, Y/2] = iZ/2, \quad [Y/2, Z/2] = iX/2, \quad [Z/2, X/2] = iY/2. \quad (4.12)$$

Thus, we can construct an $\text{SU}(2)$ subgroup by exponentiating the generators (4.11). Let us denote this subgroup by G .

Now, let us put

$$\begin{aligned} \Omega_i &= J(t_i - t_{i-1})/2, \\ W^i &= \Omega_i (\cos \phi_i X + \sin \phi_i Y)/2 = e^{-i\phi_i Z/2} (\Omega_i X/2) e^{i\phi_i Z/2}. \end{aligned} \quad (4.13)$$

Then, we observe that

$$e^{-iW^i} = e^{-i\phi_i Z/2} e^{-i\Omega_i X/2} e^{i\phi_i Z/2} \in G. \quad (4.14)$$

Thus, for this W^i , we observe the identification between Ω_i, X, Y , and Z and $\theta_i, \sigma_x, \sigma_y$, and σ_z in Eq. (4.4), respectively. Since the J -coupling error (4.10) is

[†] Precisely speaking, $\det U_{\text{CNOT}} = -1$ and it is not an element of $\text{SU}(4)$. Nevertheless, we can multiply this matrix by an unphysical phase $e^{i\pi/4}$ to make it an element of $\text{SU}(4)$. Two quantum gates that differ by an overall phase will be identified hereafter.

equivalent to the pulse length error (4.5) under this identification, we can construct a “composite pulse”, which is robust against the J -coupling error, if we merely replace $\theta_i, \sigma_x, \sigma_y$, and σ_z by Ω_i, X, Y , and Z , respectively. In fact, as stated before, such composite pulses based on the identification have been proposed in [17, 18, 19, 20]. One of these composite pulses shall be examined later. Composite pulses designed under this identification are GQGs, since this identification keeps the mathematical structure of the theory unchanged.

Two remarks are in order. First, the definition of Z tells us that we can freely tune the parameter ϕ_i by changing the rf-field along the y -axis of the second qubit. Second, we can define the Bloch sphere for an orbit generated by G and $|\psi\rangle \in \mathbb{C}^{2 \otimes 2}$ if $|\psi\rangle$ is an eigenvector of some element $U \in G$. In other words, if there exists $U \in G$ such that

$$U |\psi\rangle = e^{i\gamma} |\psi\rangle, \quad (4.15)$$

then the G -orbit $G|\psi\rangle$ of $|\psi\rangle$ is identified as the Bloch sphere S^2 . This observation ensures that we can visualise the time evolution of a cyclic state associated with $U \in G$ as a trajectory in the Bloch sphere, as long as we use the composite pulses proposed so far.

5. Examples of Geometric Composite Pulse

In this section, we give several examples demonstrating our claim that two types of composite pulses introduced in the previous section are GQGs. To this end, we shall evaluate the dynamical phase of several composite pulses and verify that the dynamical phase indeed vanishes in all cases.

(a) One-Qubit System

We parametrise our target U as

$$U = \exp(-i\theta \mathbf{n} \cdot \boldsymbol{\sigma}/2), \quad \mathbf{n} = (\cos \phi, \sin \phi, 0). \quad (5.1)$$

Then, from Sec. 2, a cyclic state $|\psi_a\rangle$ associated with U is given as an eigenvector of U , that is,

$$|\psi_a\rangle = |(-1)^a \mathbf{n}\rangle, \quad a = 0, 1, \quad (5.2)$$

where $|(-1)^a \mathbf{n}\rangle$ is the eigenstate of $\mathbf{n} \cdot \boldsymbol{\sigma}$ such that

$$\mathbf{n} \cdot \boldsymbol{\sigma} |(-1)^a \mathbf{n}\rangle = (-1)^a |(-1)^a \mathbf{n}\rangle. \quad (5.3)$$

We shall often use the following useful formula:

$$\langle \mathbf{n} | \mathbf{m} \cdot \boldsymbol{\sigma} | \mathbf{n} \rangle = \mathbf{n} \cdot \mathbf{m}. \quad (5.4)$$

Note that the vector \mathbf{n} is the Bloch vector for the state $|\mathbf{n}\rangle$ and we have

$$U |(-1)^a \mathbf{n}\rangle = \omega_a |(-1)^a \mathbf{n}\rangle, \quad \omega_a = \exp[(-1)^{a+1} i\theta/2]. \quad (5.5)$$

All composite pulses, for which we evaluate the dynamical phases, are composed from $k = 2l - 1$ pulses, which satisfy the ‘time-symmetric’ condition

$$W^i = W^{k+1-i}. \quad (5.6)$$

Many implications of this condition are found in [5]. Now we address that this condition leads to

$$\gamma_d^a(i) = \gamma_d^a(k+1-i). \quad (5.7)$$

See Appendix B for the proof. Hence, the dynamical phase is rewritten as

$$\gamma_d^a = 2[\gamma_d^a(1) + \cdots + \gamma_d^a(l-1)] + \gamma_d^a(l) \quad (5.8)$$

for a composite pulse, which is made of $k = 2l - 1$ pulses.

(i) 90° - 180° - 90° pulse

The first composite pulse was proposed by Levitt and Freeman in 1979 based on a trajectory on the Bloch sphere [4]. This is a $k = 3$ symmetric composite pulse defined by

$$\theta_1 = \theta_2/2 = \theta_3 = \pi/2, \quad \phi_1 = \phi_3 = 0, \quad \phi_2 = \pi/2. \quad (5.9)$$

We immediately find

$$W_1 = W_3 = (\pi/4)\hat{\mathbf{x}} \cdot \boldsymbol{\sigma}, \quad W_2 = (\pi/2)\hat{\mathbf{y}} \cdot \boldsymbol{\sigma}, \quad (5.10)$$

which leads to

$$U = e^{-iW_1}e^{-iW_2}e^{-iW_1} = -i\sigma_y. \quad (5.11)$$

Hence, we observe that the target is fixed to $\theta = \pi$ and $\phi = \pi/2$ and there are no free parameters we may adjust. It follows from Eq. (5.11) that $|\psi_a\rangle = |(-1)^a\hat{\mathbf{y}}\rangle$.

Let us proceed to the calculation of the dynamical phase. First, we have

$$\gamma_d^a(1) = -(\pi/4) \langle (-1)^a\hat{\mathbf{y}} | \hat{\mathbf{x}} \cdot \boldsymbol{\sigma} | (-1)^a\hat{\mathbf{y}} \rangle = (-1)^{a+1}(\pi/4)\hat{\mathbf{x}} \cdot \hat{\mathbf{y}} = 0 \quad (5.12)$$

from the formula (5.4). Next, we observe

$$|\psi_a(1)\rangle = e^{-iW^1} |\psi_a\rangle = e^{-i\pi\sigma_x/4} |(-1)^a\hat{\mathbf{y}}\rangle = |(-1)^a\hat{\mathbf{z}}\rangle \quad (5.13)$$

to obtain

$$\gamma_d^a(2) = -(\pi/2) \langle (-1)^a\hat{\mathbf{z}} | \hat{\mathbf{y}} \cdot \boldsymbol{\sigma} | (-1)^a\hat{\mathbf{z}} \rangle = (-1)^{a+1}(\pi/2)\hat{\mathbf{y}} \cdot \hat{\mathbf{z}} = 0. \quad (5.14)$$

Summing up these, we reach

$$\gamma_d^a = 2\gamma_d^a(1) + \gamma_d^a(2) = 0. \quad (5.15)$$

We can confirm Eq. (5.7) by further calculation. We find

$$|\psi_a(2)\rangle = e^{-iW^2} e^{-iW^1} |\psi_a\rangle = e^{-iW^2} |(-1)^a\hat{\mathbf{z}}\rangle = |(-1)^{a+1}\hat{\mathbf{z}}\rangle, \quad (5.16)$$

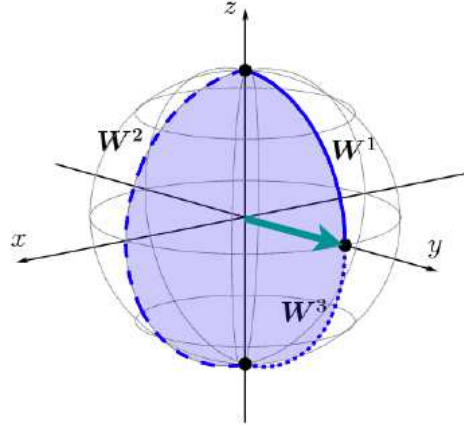


Figure 1. (Colour online) Excursion of the cyclic state $|\hat{\mathbf{y}}\rangle$ under the 90° - 180° - 90° pulse on the Bloch sphere. The green arrow is the Bloch vector of the cyclic state. The solid angle of the blue area enclosed by the trajectory of the Bloch vector is equal to $\pi = \theta$, which also shows that this composite pulse is a GQG (See Appendix A).

from which it follows that

$$\gamma_d^a(3) = -(\pi/4) \langle (-1)^{a+1} \hat{\mathbf{z}} | \hat{\mathbf{x}} \cdot \boldsymbol{\sigma} | (-1)^{a+1} \hat{\mathbf{z}} \rangle = (-1)^a (\pi/4) \hat{\mathbf{x}} \cdot \hat{\mathbf{z}} = 0 = \gamma_d^a(1). \quad (5.17)$$

The time-evolution of the cyclic states ends up with

$$|\psi_a(3)\rangle = e^{-iW^3} |\psi_a(2)\rangle = |(-1)^a \hat{\mathbf{y}}\rangle = |\psi_a\rangle, \quad (5.18)$$

as expected. These results are summarised as

$$|\pm \hat{\mathbf{y}}\rangle \xrightarrow{e^{-iW^1}} |\pm \hat{\mathbf{z}}\rangle \xrightarrow{e^{-iW^2}} |\mp \hat{\mathbf{z}}\rangle \xrightarrow{e^{-iW^3}} |\pm \hat{\mathbf{y}}\rangle, \quad \gamma_d^a(i) = 0. \quad (5.19)$$

See Fig. 1 for the graphical representation of this excursion.

The lesson we learn from this composite pulse is that the converse of our statement is not always true: Not all GQGs for a spin-1/2 system are Type A composite pulses robust against the pulse length error. Indeed, this pulse is of Type B since $\Delta W \neq 0$. This has been overlooked in [36].

(ii) SCROFULOUS

SCROFULOUS is a $k = 3$ time-symmetric composite pulse constructed by Cummins, Llewellyn and Jones [21]. This composite pulse was designed by using perturbation theory and quaternion algebra. Given a target (5.1), SCROFULOUS takes the form

$$\begin{aligned} \theta_1 = \theta_3 &= \text{arcsinc}[2 \cos(\theta/2)/\pi], & \theta_2 &= \pi \\ \phi_1 = \phi_3 &= \phi + \arccos[-\pi \cos \theta_1 / (2\theta_1 \sin(\theta/2))], \\ \phi_2 &= \phi_1 - \arccos[-\pi / (2\theta_1)], \end{aligned} \quad (5.20)$$

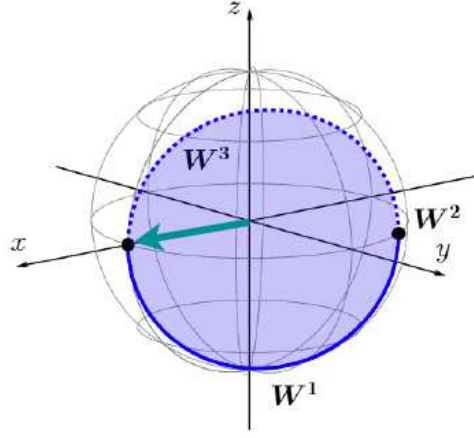


Figure 2. (Colour online) Excursion of the cyclic state $|\hat{\mathbf{x}}\rangle$ of the SCROFULOUS for a target $\theta = \pi, \phi = 0$ on the Bloch sphere. The green arrow is the Bloch vector of the cyclic state. The state $e^{-iW^1}|\hat{\mathbf{x}}\rangle$ pauses during the application of the pulse W^2 , since it is an eigenstate of the pulse W^2 . The solid angle of the blue area is equal to θ ; this composite pulse is a GQG.

where $\text{sinc } x = \sin x/x$. Note that SCROFULOUS implements any one-qubit unitary operator of the form (5.1).

Let us evaluate the dynamical phase. We set $\phi = 0$ for simplicity, while extension to an arbitrary ϕ is straightforward. First, we have

$$\gamma_d^a(1) = -\theta_1 \langle (-1)^a \mathbf{n} | \mathbf{n}_1 \cdot \boldsymbol{\sigma} / 2 | (-1)^a \mathbf{n} \rangle = (-1)^{a+1} \theta_1 \mathbf{n} \cdot \mathbf{n}_1 / 2 = (-1)^{a+1} (\theta_1 / 2) \cos \phi_1. \quad (5.21)$$

Next, observe that

$$V^{1\dagger} W^2 V^1 = \frac{\theta_2}{2} [\cos^2(\theta_1/2) \mathbf{n}_2 + \sin^2(\theta_1/2) \mathbf{m} - \sin \theta_1 (\mathbf{n}_1 \times \mathbf{n}_2)] \cdot \boldsymbol{\sigma}, \quad (5.22)$$

where

$$\mathbf{m} = 2(\mathbf{n}_2 \cdot \mathbf{n}_1) \mathbf{n}_1 - \mathbf{n}_2. \quad (5.23)$$

Since we have

$$\begin{aligned} \mathbf{n}_2 \cdot \mathbf{n} &= \cos \phi_2 = -\pi \cos \phi_1 / (2\theta_1) + \sin \phi_1 \sin[\arccos(-\pi/(2\theta_1))], \\ \mathbf{m} \cdot \mathbf{n} &= \cos(2\phi_1 - \phi_2) = -\pi \cos \phi_1 / (2\theta_1) - \sin \phi_1 \sin[\arccos(-\pi/(2\theta_1))], \\ (\mathbf{n}_1 \times \mathbf{n}_2) \cdot \mathbf{n} &= 0, \end{aligned} \quad (5.24)$$

we observe

$$\begin{aligned} \gamma_d^a(2) &= -\langle \psi_a | V^{1\dagger} W^2 V^1 | \psi_a \rangle \\ &= (-1)^a (\pi/2) \{ (\pi/(2\theta_1)) \cos \phi_1 + \cos \theta_1 \sin[\arccos(-\pi/(2\theta_1))] \sin \phi_1 \}. \end{aligned} \quad (5.25)$$

Using $\sin(\arccos x) = \sqrt{1-x^2}$ and

$$\sin \phi_1 = \sqrt{1 - (\pi/(4\theta_1))^2} / \sin(\theta/2), \quad (5.26)$$

we immediately derive

$$\begin{aligned} \gamma_d^a &= 2\gamma_d^a(1) + \gamma_d^a(2) \\ &= (-1)^a \{ \theta_1 [1 - (\pi/(2\theta_1))^2] \cos \phi_1 + (\pi/2) \cos \theta_1 \sin[\arccos(-\pi/(2\theta_1))] \sin \phi_1 \} \\ &= (-1)^a [1 - (\pi/(2\theta_1))^2] [\theta_1 \cos \phi_1 + \pi \cos \theta_1 / (2 \sin(\theta/2))] \\ &= 0. \end{aligned} \quad (5.27)$$

Hence SCROFULOUS is a GQG. The trajectory of the cyclic state is given in Fig. 2.

(iii) *Broad Band 1 (BB1)*

Now we turn to the BB1, which was proposed by Wimperis [39]. For brevity's sake, we treat a $k = 5$ time-symmetric variant of the BB1 sequence. We call this variant time-symmetric BB1. The BB1 pulse sequence is useful for the implementation of QIP, since it compensates for the pulse length error up to the second order in perturbative expansion [16]. There are two techniques to generalise the BB1 pulse sequence [22]. Using these techniques, we can design a composite pulse sequence, which compensates for the pulse length error up to an arbitrary higher order in perturbative expansion.

For a target (5.1) with angles θ and ϕ , the time-symmetric BB1 consists of

$$\begin{aligned} \theta_1 = \theta_5 = \theta/2, \quad \theta_2 = \theta_3/2 = \theta_4 = \pi, \\ \phi_1 = \phi_5 = \phi, \quad \phi_2 = \phi_4 = \phi + \kappa, \quad \phi_3 = 3\phi + \kappa, \end{aligned} \quad (5.28)$$

with

$$\kappa = \arccos[-\theta/(4\pi)]. \quad (5.29)$$

Let us evaluate the dynamical phase associated with the time-symmetric BB1. First, we note from $U = e^{-2iW^1}$ that

$$V^1 |\psi_a\rangle = e^{-iW^1} |\psi_a\rangle = \pm \sqrt{\omega_a} |\psi_a\rangle. \quad (5.30)$$

Then, we have

$$\gamma_d^a(1) = -\langle \psi_a | W^1 | \psi_a \rangle = (-1)^{a+1} \theta_1 \mathbf{n}_1 \cdot \mathbf{n}/2 = (-1)^{a+1} \theta/4. \quad (5.31)$$

Next we find from $\theta_2 = \pi$ and $\phi_2 = \phi + \kappa$ that

$$\gamma_d^a(2) = -\langle \psi_a | V^{1\dagger} W^2 V^1 | \psi_a \rangle = -\langle \psi_a | W^2 | \psi_a \rangle = (-1)^{a+1} \pi \mathbf{n}_2 \cdot \mathbf{n}/2 = (-1)^a \theta/8 \quad (5.32)$$

and

$$e^{-iW^2} |\psi_a\rangle = |(-1)^a \mathbf{n}'\rangle; \quad \mathbf{n}' = (\cos(\phi + 2\kappa), \sin(\phi + 2\kappa), 0). \quad (5.33)$$

This leads to

$$\gamma_d^a(3) = -\langle \psi_a | V^{2\dagger} W^3 V^2 | \psi_a \rangle = (-1)^{a+1} \pi \mathbf{n}_3 \cdot \mathbf{n}' = (-1)^a \theta/4. \quad (5.34)$$

By adding individual dynamical phases, we finally obtain

$$\gamma_d^a = 2\gamma_d^a(1) + 2\gamma_d^a(2) + \gamma_d^a(3) = (-1)^{a+1} (\theta/2 - \theta/4 - \theta/4) = 0. \quad (5.35)$$

This result confirms that the time-symmetric BB1 is also a GQG.

(iv) *Knill's sequence*

Knill's sequence [40, 41] is a $k = 5$ time-symmetric composite pulse. This sequence implements the target U given by

$$\theta = \pi, \quad \mathbf{n} = (\cos(\alpha - \pi/6), \sin(\alpha - \pi/6), 0) \quad (5.36)$$

where α is a free parameter. The sequence is defined by

$$\theta_i = \pi \ (1 \leq i \leq 5), \quad \phi_1 = \phi_5 = \alpha + \pi/6, \quad \phi_2 = \phi_4 = \alpha, \quad \phi_3 = \alpha + \pi/2. \quad (5.37)$$

This sequence is used in experiments to maintain the coherence of nitrogen-vacancy centres in diamond [40] and to decouple a system from the environment [41]. Note that this sequence is robust against not only the pulse length error, but also the off-resonance error [41].

Let us calculate the dynamical phase. First, we have

$$\gamma_d^a(1) = -\langle \psi_a | W^1 | \psi_a \rangle = (-1)^{a+1} \pi \mathbf{n}_1 \cdot \mathbf{n} / 2 = (-1)^{a+1} (\pi/2) \cos(\pi/3) = (-1)^{a+1} \pi/4. \quad (5.38)$$

We find $V^1 | \psi_a \rangle = |(-1)^a \mathbf{n}' \rangle$ with

$$\mathbf{n}' = (\cos(\alpha + \pi/2), \sin(\alpha + \pi/2), 0). \quad (5.39)$$

Then, by the similar argument as that used for the first step, we have

$$\gamma_d^a(2) = 0. \quad (5.40)$$

Further, we observe $V^2 | \psi_a \rangle = |(-1)^a \mathbf{n}'' \rangle$ with

$$\mathbf{n}'' = (\cos(\alpha - \pi/2), \sin(\alpha - \pi/2), 0). \quad (5.41)$$

Then, we have

$$\gamma_d^a(3) = (-1)^a \pi/2. \quad (5.42)$$

We find, by adding individual dynamical phases,

$$\gamma_d^a = 2\gamma_d^a(1) + 2\gamma_d^a(2) + \gamma_d^a(3) = (-1)^{a+1} (\pi/2 + 0 - \pi/2) = 0. \quad (5.43)$$

This example shows that the composite pulses robust against several systematic errors are also GQGs, if they compensates for at least the pulse length error. Thus, by construction, the composite pulses proposed in [10, 23], which are simultaneously robust against the above two errors, are also GQGs.

(b) *Two-Qubit System*

Since our interest lies in the CNOT operation, we choose the target

$$U = e^{-i\Omega X/2}, \quad (5.44)$$

which is the entangling part in the CNOT gate. The cyclic state $|\psi_a \rangle$ is an eigenstate of X in Eq. (4.11). In the binary notation $a = 2p + q$ where $p, q \in \{0, 1\}$, we find

$$|\psi_a \rangle = |p \rangle \otimes |q \rangle. \quad (5.45)$$

Jones designed a composite pulse sequence for a two-qubit system from a one-qubit composite pulse sequence [17], by employing the isomorphism among the generators given in Sec. 4 (b). Let us introduce a notation $(\Omega)_\phi = \exp[-i\Omega(\cos\phi X + \sin\phi Y)/2]$ and set the target to $(\pi/2)_0$ in this notation. Jones' sequence is given by

$$(\pi/4)_0(\pi)_\kappa(2\pi)_{3\kappa}(\pi)_\kappa(\pi/4)_0, \quad \kappa = \arccos(-1/8). \quad (5.46)$$

Since the isomorphism maps X , Y , and Z to the Pauli matrices σ_x , σ_y , and σ_z , respectively, Jones' sequence is a two-qubit analogue of the BB1 sequence: the combination of the first and last pulses is the target pulse ($\theta = \pi/2$, $\phi = 0$) and the others are the same as the BB1 sequence (5.28). Similarly, the composite pulses in [18, 19, 20] are the two-qubit counterparts of those in [22].

Evaluation of the dynamical phase is easy if we make use of the isomorphism already mentioned. Since X is mapped to σ_x , the cyclic vector $|p\rangle \otimes |q\rangle$ should be sent to $|(-1)^{p+q}\hat{x}\rangle$, which is also an eigenvector of the target $U = \exp(-i\pi\sigma_x/4)$. Thus the dynamical phase of Jones' sequence is transferred to that of the BB1 sequence, which leads to

$$\gamma_d^a = 0, \quad (5.47)$$

showing the sequence has vanishing dynamical phase. One can also achieve the same result by direct calculation without employing the isomorphism.

6. Two Composite z -Rotations

In NMR, rotations around the z -axis must be implemented by a sequence of pulses, since the rf-pulses (4.4) have the restriction $\mathbf{n}_i \perp \hat{\mathbf{z}}$. Thus, it is of interest to investigate whether the sequences are geometric.

First, we consider the following $k = 3$ sequence to realise a target $U = e^{-i\theta\sigma_z/2}$:

$$\theta_1 = \theta_3 = \pi/2, \quad \theta_2 = \theta, \quad \phi_1 = -\phi_3 = \pi/2, \quad \phi_2 = 0. \quad (6.1)$$

The cyclic states are $|\psi_a\rangle = |(-1)^a\hat{\mathbf{z}}\rangle = |a\rangle$. Let us calculate the dynamical phase. The first one is

$$\gamma_d^a(1) = -(\pi/4) \langle \psi_a | \hat{\mathbf{y}} \cdot \boldsymbol{\sigma} | \psi_a \rangle = (-1)^{a+1}(\pi/4) \hat{\mathbf{y}} \cdot \hat{\mathbf{z}} = 0. \quad (6.2)$$

We find $V^1 |\psi_a\rangle = |(-1)^a\hat{\mathbf{x}}\rangle$, which leads to

$$\gamma_d^a(2) = -(\theta/2) \langle (-1)^a\hat{\mathbf{x}} | \hat{\mathbf{x}} \cdot \boldsymbol{\sigma} | (-1)^a\hat{\mathbf{x}} \rangle = (-1)^{a+1}\theta/2. \quad (6.3)$$

Furthermore, we obtain $V^2 |\psi_a\rangle = \exp[(-1)^{a+1}i\theta/2] |(-1)^a\hat{\mathbf{x}}\rangle$. Thus, we observe

$$\gamma_d^a(3) = (\pi/4) \langle (-1)^a\hat{\mathbf{x}} | \hat{\mathbf{y}} \cdot \boldsymbol{\sigma} | (-1)^a\hat{\mathbf{x}} \rangle = (-1)^a(\pi/4) \hat{\mathbf{y}} \cdot \hat{\mathbf{x}} = 0. \quad (6.4)$$

We conclude

$$\gamma_d^a = (-1)^{a+1}\theta/2 \neq 0. \quad (6.5)$$

Hence the pulse sequence (6.1) is not a GQG. Note that this sequence is not robust against the pulse length error, that is, $\Delta W \neq 0$, which is exactly the contraposition of our claim.

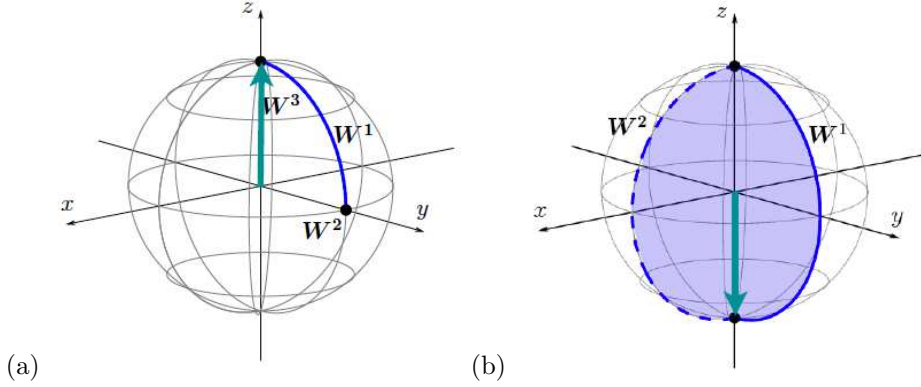


Figure 3. (Colour online) Excursions of the cyclic states on the Bloch sphere. (a) The trajectory of the cyclic state $|\hat{z}\rangle$ under the pulse sequence (6.1). Note that the trajectory fails to close, which shows that this sequence is dynamical. (b) The trajectory of the cyclic state $|\hat{-z}\rangle$ under the pulse sequence (6.6) for $\theta = \pi$. The solid angle subtended by the trajectory of the Bloch vector is $\pi = \theta$, which shows the geometric nature of the sequence.

Second, we investigate a $k = 2$ pulse for $U = e^{i\theta\sigma_z/2}$:

$$\theta_1 = \theta_2 = \pi, \quad \phi_1 = 0, \quad \phi_2 = \theta/2. \quad (6.6)$$

The cyclic states are the same as those of the previous sequence. We have

$$\gamma_d^a(1) = -(\pi/2) \langle \psi_a | \hat{x} \cdot \sigma | \psi_a \rangle = (-1)^{a+1} (\pi/2) \hat{x} \cdot \hat{z} = 0. \quad (6.7)$$

By the same way, we compute

$$\gamma_d^a(2) = 0, \quad (6.8)$$

which clearly shows

$$\gamma_d^a = 0. \quad (6.9)$$

Hence the pulse sequence (6.6) is a GQG. This pulse is not robust against the pulse length error. Indeed, we may check

$$\Delta W = \epsilon \frac{\pi}{2} \left[\left(1 + \cos \frac{\theta}{2} \right) \sigma_x - \sin \frac{\theta}{2} \sigma_y \right] \neq 0 \quad (6.10)$$

by direct calculation. This also tells us that not all GQGs are robust against the pulse length error. The difference of these two composite z -rotations are visualised in Fig. 3.

7. Conclusion and Discussions

In this article, we uncovered the relation between GQGs and the composite pulses robust against certain kinds of systematic errors. For the error (4.1), proportional

to the Hamiltonian times the operation time, the compensation of the error automatically leads to vanishing dynamical phase. Thus, a non-trivial operation by a composite pulse robust against such an error is a GQG.

We pointed out that there are two kinds of errors assuming the form (4.1). One is the pulse length error and the other is the J -coupling error. This implies that the composite pulses robust against these errors are GQGs. This observation was illustrated and confirmed by directly showing that the dynamical phase vanishes for several typical composite pulses: 90° - 180° - 90° , SCROFULOUS, BB1, Knill's sequence for the pulse length error and Jones' pulse sequence for the J -coupling error. The two most common composite z -rotations were also examined.

Our work has shown that we can construct a universal gate set composed of GQGs simply by using the composite pulses. This suggests that NMR is quite a useful test bench of geometric quantum computation. In view of this, further study of composite pulses, *e.g.* [37], is desirable for deeper understanding of the geometric quantum computation.

We would like to thank Jonathan A. Jones and Yukihiro Ota for valuable discussions and Dieter Suter for drawing our attention to Knill's sequence. This work is supported by 'Open Research Center' Project for Private Universities: matching fund subsidy from MEXT (Ministry of Education, Culture, Sports, Science and Technology), Japan. YK and MN would like to thank partial supports of Grants-in-Aid for Scientific Research from the JSPS (Grant No. 23540470).

Appendix A. Geometry of Aharonov-Anandan Phase

In this appendix, we outline the relevant aspects of the Aharonov-Anandan phase in the context of the present article. The geometric nature of the Aharonov-Anandan phase is derived from that of the fibre bundle structure associated with the Hilbert space. See [13, 32] for technical details.

Consider the Hilbert space \mathbb{C}^n . In quantum mechanics, we are exclusively concerned with the set of normalised vectors in \mathbb{C}^n . The set of normalised vectors form the $(2n-1)$ -dimensional sphere $S^{2n-1} \subset \mathbb{C}^n$. Moreover, we need to identify vectors that differ by an overall phase; two normalised states $|\psi\rangle$ and $e^{i\gamma}|\psi\rangle$ represent the identical physical state for any $\gamma \in \mathbb{R}$. The manifold obtained from S^{2n-1} under this identification is called the complex projective space;

$$\mathbb{C}P^{n-1} \simeq S^{2n-1}/U(1),$$

where $U(1)$ is the set of overall phases.

For $n = 2$, we obtain $\mathbb{C}P^1 = S^2$, which is nothing but the Bloch sphere. Accordingly, S^3 is identified with a $U(1)$ -bundle over S^2 (the Hopf fibration). More generally, S^{2n-1} is a $U(1)$ -bundle over the base manifold $\mathbb{C}P^{n-1}$. A point in $\mathbb{C}P^{n-1}$ represents a physical state and its phase freedom is represented by the fibre $U(1)$. The identification naturally introduces the projection $\pi : S^{2n-1} \rightarrow \mathbb{C}P^{n-1}$. Fixing the phase is equivalent to taking a point in the fibre (See Fig. 4).

It should be noted that $\mathbb{C}P^{n-1}$ has a natural metric called the Fubini-Study metric. Given a metric in the base manifold, we can construct a connection in the base manifold. This defines the horizontal lift of a given curve in the base manifold to the fibre bundle S^{2n-1} . Now suppose that there is a closed loop in the base manifold. If one carries a point on a fibre over $p \in \mathbb{C}P^{n-1}$ along the horizontal lift

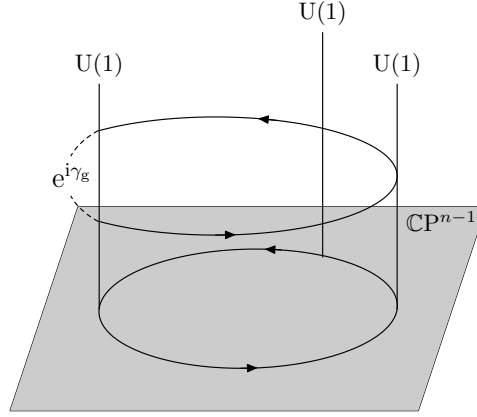


Figure 4. Schematic diagram of Aharonov-Anandan phase. The set of the normalised states forms $S^{2n-1} \subset \mathbb{C}^n$ and this subset S^{2n-1} can be seen as a $U(1)$ -bundle over the projective Hilbert space \mathbb{CP}^{n-1} . Given a closed path in the base manifold \mathbb{CP}^{n-1} , the horizontal lift of the path is naturally defined by a connection in the $U(1)$ -bundle. The holonomy associated with the horizontal lift is given as $e^{i\gamma_g} \in U(1)$, which can be seen as a global phase difference accumulated through the parallel transport along the horizontal lift on the path in \mathbb{CP}^{n-1} .

of the loop, the point comes back to a point in the same fibre, which is not necessary the initial point. This $U(1)$ phase factor obtained after traversing a loop is called the holonomy associated with the loop and the horizontal lift. The Aharonov-Anandan phase is nothing but this $U(1)$ phase factor, which is geometric in the sense that it depends only on the loop in the base manifold and the connection of the $U(1)$ -bundle but not on how fast the loop is traversed.

We note that the twice the Aharonov-Anandan phase is the solid angle at the origin subtended by the trajectory of a state vector on the Bloch sphere (\mathbb{CP}^1 , in this case) during a 1-qubit operation.

Appendix B. Proof of Eq. (5.7)

In this appendix we prove Eq. (5.7). For this purpose, we first note the identity

$$\sigma_z W^i \sigma_z = -W^i \quad (\text{B } 1)$$

for W^i of Eq. (4.4), because $\mathbf{n}_i \perp \hat{\mathbf{z}}$. Multiplying $-i$ and exponentiating Eq. (B 1), we find

$$\sigma_z e^{-iW^i} \sigma_z = e^{iW^i}. \quad (\text{B } 2)$$

Then, we obtain

$$V^{k-i} = e^{iW^i} \cdots e^{iW^1} U = \sigma_z V^i \sigma_z U \quad (\text{B } 3)$$

for a time-symmetric composite pulse. It then follows that

$$\begin{aligned}
 |\psi_a(k-i)\rangle &= V^{k-i} |\psi_a\rangle \\
 &= \sigma_z V^i \sigma_z U |\psi_a\rangle && \text{from Eq. (B 3)} \\
 &= \omega_a \sigma_z V^i \sigma_z |\psi_a\rangle && \text{from Eq. (5.5)} \\
 &= \omega_a \sigma_z V^i |\psi_{a\oplus 1}\rangle \\
 &= \omega_a \sigma_z |\psi_{a\oplus 1}(i)\rangle,
 \end{aligned} \tag{B 4}$$

where we denote the sum modulo two by \oplus . Therefore, using the condition $\text{Tr } W^i = 0$ and the completeness relation with respect to $\{|\psi_a(i)\rangle\}_{a=1,2}$, we observe that

$$\begin{aligned}
 \gamma_d^a(k+1-i) &= -\langle \psi_a(k-i) | W^{k+1-i} | \psi_a(k-i) \rangle \\
 &= -\langle \psi_{a\oplus 1}(i) | \sigma_z W^i \sigma_z | \psi_{a\oplus 1}(i) \rangle && \text{from Eq. (B 4) and } |\omega_a|^2 = 1 \\
 &= \langle \psi_{a\oplus 1}(i) | W^i | \psi_{a\oplus 1}(i) \rangle && \text{from Eq. (B 1)} \\
 &= \text{Tr} [W^i (\mathbb{1}_2 - |\psi_a(i)\rangle \langle \psi_a(i)|)] \\
 &= -\langle \psi_a(i) | W^i | \psi_a(i) \rangle && \text{from } \text{Tr } W^i = 0 \\
 &= -\langle \psi_a(i-1) | W^i | \psi_a(i-1) \rangle \\
 &= \gamma_d^a(i),
 \end{aligned} \tag{B 5}$$

which proves Eq. (5.7).

References

- [1] Freeman, R. 1999 *Spin Choreography*. Oxford: Oxford University Press.
- [2] Claridge, T. D. W. 1999 *High-Resolution NMR Techniques in Organic Chemistry*. Oxford: Elsevier.
- [3] Jones, J. A. 2009 Composite pulses in NMR quantum computation. *J. Ind. Inst. Sci.* **89**, 303-308.
- [4] Levitt, M. H. & Freeman, R. 1979 NMR Population Inversion Using a Composite Pulse. *J. Magn. Reson.* **33**, 473-476. (doi: 10.1016/0022-2364(79)90265-8)
- [5] Levitt, M. H. 1986 Composite Pulses. *Prog. NMR Spectrosc.* **18**, 61-122. (doi: 10.1016/0079-6565(86)80005-X)
- [6] Levitt, M. H. 1996 Composite Pulses. In *Encyclopedia of Nuclear Magnetic Resonance* (eds. D. M. Grant and R. K. Harris), pp. 1396-1411. Sussex: Wiley.
- [7] Tycko, R., Pines, A. & Guckenheimer J. 1985 Fixed point theory of iterative excitation schemes in NMR. *J. Chem. Phys.* **83**, 2775-2802. (doi: 10.1063/1.449228)
- [8] Khaneja, N., Reiss, T., Kehlet, C., Schulte-Herbrüggen, T. & Glaser, S. J. 2005 Optimal control of coupled spin dynamics: design of NMR pulse sequences by gradient ascent algorithms. *J. Magn. Reson.* **172**, 296-305. (doi: 10.1016/j.jmr.2004.11.004)

- [9] Machnes, S., Sander, U., Glaser, S. J., de Fouquières P., Gruslys, A., Schirmer, S. & Schulte-Herbrüggen, T. 2011 Comparing, optimizing, and benchmarking quantum-control algorithms in a unifying programming framework. *Phys. Rev. A* **84**, 022305. (doi: 10.1103/PhysRevA.84.022305)
- [10] Ichikawa, T., Bando, M., Kondo, Y. & Nakahara, M. 2011 Designing Robust Unitary Gates: Application to Concatenated Composite Pulse. *Phys. Rev. A* **84**, 062311. (doi: 10.1103/PhysRevA.84.062311)
- [11] Barenco, A., Bennett, C. H., Cleve, R., DiVincenzo, D. P., Margolus, N., Shor, P., Sleator, T., Smolin, J. A. & Weinfurter, H. 1995 Elementary gates for quantum computation. *Phys. Rev. A* **52**, 3457-3467. (doi: 10.1103/PhysRevA.52.3457)
- [12] Nielsen, M. A. & Chuang, I. C. 2000 *Quantum Information and Quantum Computation*. Cambridge: Cambridge University Press.
- [13] Bengtsson, I. & Życzkowski, K. 2006 *Geometry of Quantum States*, New York: Cambridge University Press.
- [14] Gaitan, F. 2008 *Quantum Error Correction and Fault Tolerant Quantum Computing*. Boca Raton: Taylor & Francis.
- [15] Nakahara, M. & Ohmi, T. 2008 *Quantum Computing: From Linear Algebra to Physical Realizations*. Boca Raton: Taylor & Francis.
- [16] Jones, J. A. 2011 Quantum Computing with NMR. *Prog. NMR Spectrosc.* **59**, 91-120. (doi: 10.1016/j.pnmrs.2010.11.001)
- [17] Jones, J. A. 2003 Robust Ising Gates for Practical Quantum Computation. *Phys. Rev. A* **67**, 012317. (doi: 10.1103/PhysRevA.67.012317)
- [18] Hill, C. D. 2007 Robust Controlled-NOT Gates from Almost Any Interaction. *Phys. Rev. Lett.* **98**, 180501. (doi: 10.1103/PhysRevLett.98.180501)
- [19] Testolin, M. J., Hill, C. D., Wellard, C. J. & Hollenberg, L. C. L. 2007 Robust controlled-NOT gate in the presence of large fabrication-induced variations of the exchange interaction strength. *Phys. Rev. A* **76**, 012302. (doi: 10.1103/PhysRevA.76.012302)
- [20] Tomita, Y., Merrill, J. T. & Brown, K. R. 2010 Multi-Qubit Compensation Sequences. *New J. Phys.* **12**, 015002. (doi: 10.1088/1367-2630/12/1/015002)
- [21] Cummins, H. K., Llewellyn, G. & Jones, J. A. 2003 Tackling systematic errors in quantum logic gates with composite rotations. *Phys. Rev. A* **67**, 042308. (doi: 10.1103/PhysRevA.67.042308)
- [22] Brown, K. R., Harrow, A. W., & Chuang, I. L. 2004 Arbitrarily accurate composite pulse sequences. *Phys. Rev. A* **70**, 052318. (doi: 10.1103/PhysRevA.70.052318)
- [23] Alway, W. G. & Jones, J. A. 2007 Arbitrary precision composite pulses for NMR quantum computing. *J. Magn. Reson.* **189**, 114-120. (doi: 10.1016/j.jmr.2007.09.001)

- [24] Zanardi, P. & Rasetti, M. 1999 Holonomic Quantum Computation. *Phys. Lett. A* **264**, 94-99. (doi: 10.1016/S0375-9601(99)00803-8)
- [25] Zhu, S.-L., and Wang, Z.-D., 2002 Implementation of universal quantum gates based on nonadiabatic geometric phases, *Phys. Rev. Lett.* **89** 097902. (doi: 10.1103/PhysRevLett.89.097902)
- [26] Shapere, A. & Wilczek, F. 1989 *Geometric phases in physics*, Singapore: World Scientific.
- [27] Berry, M. V. 1984 Quantal Phase Factors Accompanying Adiabatic Changes. *Proc. R. Soc. A* **392**, 45-57. (doi: 10.1098/rspa.1984.0023)
- [28] Wilczek, F. & Zee, A. 1984 Appearance of Gauge Structure in Simple Dynamical Systems. *Phys. Rev. Lett.* **52**, 2111-2114. (doi: 10.1103/PhysRevLett.52.2111)
- [29] Aharonov, Y. & Anandan, J. 1987 Phase Change during a Cyclic Quantum Evolution. *Phys. Rev. Lett.* **58**, 1593-1596. (doi: 10.1103/PhysRevLett.58.1593)
- [30] Mead C. A. 1992 The geometric phase in molecular systems. *Rev. Mod. Phys.* **64**, (1992) 51-85. (doi: 10.1103/RevModPhys.64.51)
- [31] Simon, B. 1983 Holonomy, the Quantum Adiabatic Theorem, and Berry's Phase, *Phys. Rev. Lett.* **51**, 2167-2170. (doi: 10.1103/PhysRevLett.51.2167)
- [32] Nakahara, M. 2003 *Geometry, Topology and Physics*, 2nd edn, Boca Raton: Taylor & Francis.
- [33] Page, D. N. 1987 Geometrical description of Berry's phase. *Phys. Rev. A* **36**, 3479-3481. (doi: 10.1103/PhysRevA.36.3479)
- [34] Zhu, S.-L. & Zanardi, P. 2005 Geometric quantum gates that are robust against stochastic control errors. *Phys. Rev. A* **72**, 020301. (doi: 10.1103/PhysRevA.72.020301)
- [35] Blais, A. & Tremblay, A.-M. S. 2003 Effect of noise on geometric logic gates for quantum computation. *Phys. Rev. A* **67**, 012308. (doi: 10.1103/PhysRevA.67.012308)
- [36] Kondo, Y. & Bando, M. 2011 Geometric Quantum Gates, Composite Pulses, and Trotter-Suzuki Formulas. *J. Phys. Soc. Jpn.* **80**, 054002. (doi: 10.1143/JPSJ.80.054002)
- [37] Ota, Y. & Kondo, Y. 2009 Composite pulses in NMR as nonadiabatic geometric quantum gates. *Phys. Rev. A* **80**, 024302. (doi: 10.1103/PhysRevA.80.024302)
- [38] Ota, Y., Goto, Y., Kondo, Y. & Nakahara, M. 2009 Geometric quantum gates in liquid-state NMR based on a cancellation of dynamical phases. *Phys. Rev. A* **80**, 052311. (doi: 10.1103/PhysRevA.80.052311)
- [39] Wimperis, S. 1994 Broadband, Narrowband, and Passband Composite Pulses for Use in Advanced NMR Experiments. *J. Magn. Reson. A* **109**, 221-231. (doi: 10.1006/jmra.1994.1159)

- [40] Ryan, C. A., Hodges, J. S. & Cory, D. G. 2010 Robust Decoupling Techniques to Extend Quantum Coherence in Diamond. *Phys. Rev. Lett.* **105**, 200402. (doi: 10.1103/PhysRevLett.105.200402)
- [41] Souza, A. M., Álvarez G. A. & Suter, D. 2011 Robust Dynamical Decoupling for Quantum Computing and Quantum Memory. *Phys. Rev. Lett.* **106**, 240501. (doi: 10.1103/PhysRevLett.106.240501)